

A study on thermally controlled bubble growth in a superheated liquid with a thermal non-equilibrium cavitation model based on energy balances on a fixed fluid mass

M. Nickaen, T. Jaskolka, S. Mottyll & R. Skoda
*Chair of Hydraulic Fluid Machinery,
Institute of Thermodynamics and Fluid Dynamics,
Ruhr University of Bochum, Germany*

Abstract

For high temperature liquids where the bubble growth is heat diffusion controlled, the performance of a thermal non-equilibrium bubble dynamics model is analyzed. The model is based on thermal energy balances of a single bubble within a fixed mass of fluid (elementary cell). A constant mass of undissolved air is considered in the bubble. A spatially homogeneous temperature for both the vapor–air mixture within the bubble interior and the surrounding liquid is assumed. The model accuracy is compared to the well-established Rayleigh–Plesset equation in combination with the heat transfer model by Plesset and Zwick. The results of both models agree very well. Due to the embedding of a bubble in a finite amount of surrounding liquid and its harmless numerical properties, the model is assumed to be very suitable for the straightforward implementation in 3D-CFD codes as a cavitation model which will be carried out in future work.

Keywords: thermal non-equilibrium, superheated liquids, thermally controlled bubble dynamics, multi-phase flow, cavitation model.

1 Introduction

Cavitation by local fluid evaporation and gas release has a major impact on the operation and durability of hydraulic machinery and systems because of the adverse effects it has on the performance, because of the noise it creates as well



as the damage it can do to the nearby solid surfaces. The appearance of cavitation in hydraulic systems is often reduced to the study of the dynamics of a single bubble. Besides the other bubble characteristics, its growth is of utmost significance since the maximum bubble size has a strong impact on the maximum pressure peak after its collapse. The most accurate mathematical description of the bubble dynamics in a spherical coordinate system demands the numerical solution of the system of mass, momentum, and energy conservation equations, temporally and spatially resolved, see Nigmatulin [1], Beylich [2], Matsumoto and Takemura [3]. Due to the high numerical effort of these studies, approximate numerical and theoretical solutions with simplifying assumptions for the bubble growth have been developed [4–10]. The results from these investigations suggest that the early stage of bubble growth is limited primarily by momentum interactions between the liquid and the bubble. As the bubble grows, the thermal diffusion influence becomes more important until it dominates the growth rate which is bounded by the heat diffusion in the liquid. For the thermally-controlled growth regime, the numerical and theoretical results are in a good agreement with the early experimental data of Dergarabedian [11] for liquids with low thermal conductivities and low superheats.

The exact determination of the thermal term in the Rayleigh–Plesset equation [12, 13] requires the solution of the heat diffusion equation which leads to significant difficulties due to its nonlinearities. For reduction in the complexity of the bubble growth problem, Plesset and Zwick [4], Forster and Zuber [5], and Fritz and Ende [7] consider two limiting regions of bubble growth. Plesset and Zwick [4] and Forster and Zuber [5] independently determined that the bubble growth is thermally controlled by the rate of energy which is transferred through the liquid to the vapor-liquid interface. By the assumption of a thin thermal boundary layer in the liquid surrounding the bubble, an approximate solution for the energy equation was obtained by Plesset and Zwick [4]. This solution was shown to agree very well with the experimental results provided by Dergarabedian [11] for water with low superheats at atmospheric pressure.

The solution of the Rayleigh–Plesset equation [12, 13] by the use of the Plesset–Zwick [4] approximation method shows that a first critical time t_{c1} exists, above which the thermal term starts to dominate the solution (thermally controlled region), and below that, the Rayleigh–Plesset equation may be approximated by the linear Rayleigh equation (inertially controlled region) [13]. For details see Brennen [14]. Mikic *et al.* [15] derive an interpolation formula for predicting both inertially and thermally controlled regions by assuming that the bubble growth rate is limited by the Rayleigh [13] analytic solution for small time values and the approximation by Plesset and Zwick [4] as time approaches infinity.

In common 3D-CFD cavitation models [16–18], the mass transfer rate in the transport equation for the vapor volume fraction is determined by bubble dynamics models that are based on a simplified Rayleigh–Plesset equation. Since the non-linear term in the Rayleigh–Plesset equation is the root of the numerical difficulties, its asymptotic inertia-driven approximation, the simple Rayleigh equation [13] is utilized. The Rayleigh equation neglects, besides second order

non-linear inertia term, thermal effects and therefore seems to be an unjustified simplification in particular for high-temperature fluids where thermal effects dominate the bubble growth. Therefore, in the present work we adopt a cavitation model by Iben [19, 20] which is based on pure thermo-dynamical considerations and considers thermal non-equilibrium. Due to the skip of the highly non-linear Rayleigh–Plesset equation by assuming mechanical equilibrium, this model is numerically harmless and nevertheless accurate for bubble dynamics problems that are dominated by heat transfer effect. Due to the definition of an elementary cell of fixed fluid mass, consisting of a gas–vapor bubble and surrounding liquid with spatially uniform but temporally varying temperature, we assume that the model is preferred for an implementation in a 3D-CFD solver since it essentially mimics the energy balances in a computational cell, assuming a fixed mass inside the elementary cell.

In the present study, a first evaluation of the single-bubble model by Iben [19, 20] is performed on bubble growth in high-temperature superheated liquids. We compare its results with results of the approach by Plesset and Zwick [4]. In section 2 the model formulation of the thermodynamic non-equilibrium model [19, 20] is summarized. In the subsequent section 3, the results are presented and compared to the analytical results of Mikic *et al.* [15], the approach by Plesset and Zwick [4] and experimental results of Dergarabedian [11] for bubble growth dynamics in superheated water with different amounts of superheat values. The paper is finalized with the conclusions in section 4.

2 Model summary and implementation

2.1 Model formulation and assumptions

The model has been introduced by Iben [19, 20]. We summarize the model derivation and assumptions here quite briefly and refer to it as “thermal non-equilibrium model” in what follows.

The model is based on the definition of an elementary cell (see Figure 1) with a constant amount of mass m_E which contains a single spherical bubble. The bubble contains perfectly mixed vapor and gas with mass m_V and m_G and is surrounded by liquid with the mass of m_L . The gas mass m_G is constant corresponding to the assumption that gas diffusion is very slow in comparison with the evaporation process. The mass fraction of vapor μ and of undissolved gas x within the bubble are defined by $\mu = m_V/m_E$ and $x = m_G/m_E$. Assuming an ideal gas, Dalton’s law for both, air and vapor is applied and yields a relation between partial pressure of vapor and gas, p_V and p_G , and the bubble temperature T_B and its volume V . Mechanical equilibrium is assumed on the bubble wall. The Clausius–Clapeyron equation relates the vapor partial pressure to the bubble temperature for saturated conditions. The mass density of the bubble interior is calculated based on the perfect gas mixture law. For the entire elementary cell, the balance of volume change work and inner energy together with the assumption of mechanical equilibrium yield an ordinary differential equation for the spatially homogenous liquid temperature T_L [19, 20].



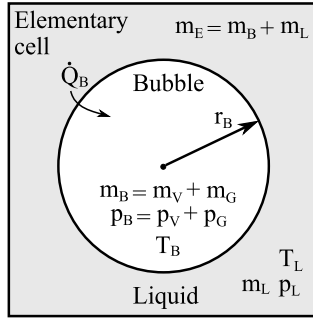


Figure 1: Elementary cell.

$$\frac{dT_L}{dt} = -\frac{1}{(1-x-\mu)c_{pL}} \left\{ (h_v - h_L + \frac{2S}{3r_B\rho_B}) \frac{d\mu}{dt} + \left[\left(\frac{c_{pG}}{c_{pv}} x + \mu \right) \frac{dh_v}{dp} - \left(\frac{x}{\rho_G} + \frac{\mu}{\rho_v} \right) - \frac{2S(x+\mu)}{3r_B\rho_B^2} \frac{d\rho_B}{dp} \right] \frac{dp_L}{dt} \right\} + \frac{T_L\alpha_L}{p_L c_{pL}} \frac{dp_L}{dt} \quad (1)$$

h_v and h_L are the specific enthalpies of the vapor and liquid. S is the liquid surface tension and c_{pG} and c_{pv} are the specific heat capacities of gas and vapor. T_L is assumed to be dependent on time only. This assumption corresponds to the neglect of the thermal boundary layer. The energy balance of the bubble relates the temporal change of inner energy to the volume change work and the heat transfer. The heat flux \dot{Q}_B from the liquid to the bubble is approximated in dependence with the temperature difference ($T_L - T_B$) by the definition of the heat transfer coefficient α_w :

$$\dot{Q}_B = \alpha_w O_B (T_L - T_B) \quad (2)$$

O_B is the bubble surface area. It is assumed that there is no relative velocity between liquid and bubble. Therefore, the convective heat transfer is neglected, and heat is only transferred by conduction within the liquid. The time-dependent heat transfer coefficient α_w is determined by equating the heat flux approximation in eqn (2) and the heat flux determined by the conduction within the liquid, proportional to the liquid temperature gradient at the interphase. The temperature gradient is approximated according to Epstein and Plesset [21], who derived an analytical relation which has also been used by Iben [20] and Klein and Iben [22]. As a result, the relation for α_w is as follows:

$$\alpha_w = \frac{\lambda_L}{r_B} + \sqrt{\frac{\rho_L c_L \lambda_L}{\pi \Delta t_k}} \quad (3)$$

and is a function of the thermal conductivity of liquid λ_L , the bubble radius r_B , the liquid density ρ_L , the specific heat capacity of liquid c_L , and the time difference between the current time of simulation t , and the start time of cavitation t_k , $\Delta t_k = (t - t_k)$. Since the liquid volume expansion coefficient α_L is small, we assume for the specific heat capacity $c_{vL} \approx c_{pL} \approx c_L$. Finally, from the energy balance on the bubble wall, an ordinary differential equation for the vapor mass fraction μ is derived [19, 20]:

$$\frac{d\mu}{dt} = \frac{3\alpha_w}{\left(h_v + \frac{2S}{3r_B\rho_B}\right)\rho_v r_B} \left(\frac{\rho_v}{\rho_G} x + \mu\right) (T_L - T_B) - \frac{1}{\left(h_v + \frac{2S}{3r_B\rho_B}\right)} \left[\left(\frac{c_{pG}}{c_{pv}} x + \mu\right) \frac{dh_v}{dp_L} - \left(\frac{x}{\rho_G} + \frac{\mu}{\rho_v}\right) - \frac{2S}{3r_B\rho_B^2} (x + \mu) \frac{d\rho_B}{dp_L} \right] \frac{dp_L}{dt} \quad (4)$$

With the geometrical relation between the bubble mass m_B and radius r_B the governing equation for the bubble radius is as follows:

$$\frac{dr_B}{dt} = \frac{m_E}{4\pi r_B^2 \rho_B} \left[\frac{d\mu}{dt} - \frac{(x+\mu)}{\rho_B} \frac{d\rho_B}{dp_L} \frac{dp_L}{dt} \right] \quad (5)$$

By applying the energy balances on both, the entire elementary cell and on the bubble, with eqns (1), (4) and (5) together with the heat transfer approximation eqns (2) and (3) as well as thermodynamic property relations a closed set of time-dependent ordinary differential equations (ODEs) is obtained, assuming that the bubble temperature T_B is known. This set of ODEs can be solved with common numerical methods. The temperature difference between liquid and bubble $T_L - T_B$ is considered to be the driving mechanism for bubble growth. While T_L is determined by eqn (1), the approximation for T_B is explained in the subsequent section.

2.2 Approximation of the bubble temperature

The bubble temperature T_B is calculated in dependence on the liquid pressure p_L assuming that the liquid is in saturation state:

$$T_B = T_{sat}(p_L) \quad (6)$$

In Figure 2, the performance of the model is illustrated for a smooth liquid pressure variation with the initial conditions $T_{L,0} = 354.5$ K, $r_{B,0} = 1.015 \times 10^{-4}$ m and $\mu_0 = 0$. The cavitation simulation starts as soon as the pressure drops below the saturation pressure at the prescribed liquid temperature. The

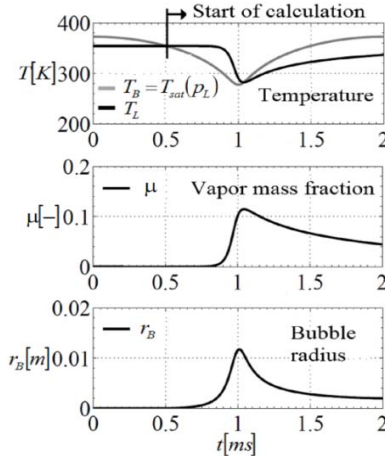


Figure 2: Bubble and liquid temperature, vapor mass fraction and bubble radius for a smooth variation of the liquid pressure.



ODE for μ , eqn (4), contains the temporal liquid pressure gradient as driving term besides the temperature difference, with opposite sign. Therefore, both driving mechanisms, liquid pressure gradient and temperature difference between liquid and bubble, compensate at the beginning of the calculation while for later instance the temperature difference dominates and causes the bubble to grow. A thermal non-equilibrium behavior is figured out because the liquid temperature, vapor mass fraction and bubble size respond with a time delay to the driving temperature difference between liquid and bubble.

2.3 Implementation of the liquid pressure evolution for superheated liquid

While the test case discussed in section 2.2 and illustrated in Figure 2 represents the principle performance of the thermal non-equilibrium model, bubble growth in superheated liquids is the test case of main interest. To implement the superheat of the liquid in the simulation, the liquid pressure drops from its initial value $p_{sat}(T_{L,0})$ instantaneously to its final value $p_{L,\infty}$. This pressure difference $p_{sat}(T_{L,0}) - p_{L,\infty}$ corresponds to the nominally prescribed superheat value. In our investigations, $p_{L,\infty}$ is the atmospheric pressure with a saturation temperature $T_{sat}(p_{L,\infty}) = 100$ °C. We approximate the pressure drop in the thermal-non equilibrium model by a short delay time τ :

$$p_L(t) = p_{L,\infty} + (p_{sat}(T_{L,0}) - p_{L,\infty}) \exp\left(-\frac{t}{\tau}\right) \quad (7)$$

The value of the delay time τ must not be exactly zero since the prescription of $p_L(t)$ must be a steady function. Preliminary calculations have revealed that for $\tau \leq 10^{-6} \times t_{c1}$, the solution does not change any more. Therefore, all presented results are obtained by $\tau = 10^{-6} \times t_{c1}$. The pressure gradient dp_L/dt comprises a very high value at the beginning of the simulation and vanishes speedily. For later instances, the solution is therefore dominated by the temperature difference rather than the pressure gradient as driving term.

2.4 Initial conditions and thermo-physical properties

Besides the initial values for $T_{L,0}$, μ_0 and $r_{B,0}$ for the ODE solver, the initial liquid mass $m_{L,0}$ and the elementary cell mass m_E need to be known and are determined as follows. From Clausius–Clapeyron equation which relates the vapor partial pressure to the bubble temperature for saturated conditions, the initial partial pressure of vapor $p_{v,0}$ within the bubble is known. Due to the assumption for the bubble temperature eqn (6), the saturation pressure equals the initial liquid pressure $p_{L,0} = p_{sat}(T_{L,0})$ in our model. As a consequence, the partial pressure of gas follows from mechanical equilibrium to $p_{G,0} = 2S/r_{B,0}$. With known $p_{v,0}$ and $p_{G,0}$ as well as the Dalton's law for both gas and vapor, the initial masses of vapor and gas within the bubble, $m_{v,0}$ and $m_{G,0}$ are determined. The definition of gas mass fraction x , section 2.1, together with its prescribed value yields the mass of the elementary cell m_E . The mass balance relations in the bubble and in the elementary cell yield the initial amount of liquid mass $m_{L,0}$.

The initial value of vapor mass fraction is determined by its definition in section 2.1. The initial mass densities of vapor and air are calculated by the respective mass and the bubble volume. The initial bubble mass density ρ_B is determined by the perfect gas mixture rule. A constant gas mass fraction $x = 10^{-8}$ is prescribed for each simulation if not otherwise stated.

For the thermo-physical property data of water, the polynomial approximation relations regarding the Helmholtz energy of substances have been used [23]. The liquid and vapor phase are assumed to be in saturated state. The data is a priori calculated by the software “Fluidcal” [24] in dependence on the liquid pressure and stored in looked-up tables. Although it is small, in eqn (1), the volume expansion coefficient α_L is evaluated according to [20] in dependence on the partial derivatives $(\partial p_L / \partial T_L)_{\rho_L}$ and $(\partial p_L / \partial \rho_L)_{T_L}$ which can directly be determined by the property software [24].

2.5 Numerical implementation

The MATLAB software [25] is used, which is a very powerful and matrix oriented high-level programming language. MATLAB contains several solvers for numerical integration of ordinary differential equations. We select the solver *ode15s* because of its accuracy and stability even for stiff ODEs. By the use of state space model principle, an n^{th} order explicit ordinary differential equation is split to n first order ordinary differential equations. The input variables are the liquid pressure $p_L(t)$ and its temporal change dp_L/dt .

3 Results and discussion

The considered test case, bubble growth in a high-temperature superheated liquid, is adopted from the measurements of Dergarabedian [11]. The first critical time t_{c1} is very low due to the high nominal temperature $T = 100^\circ\text{C}$, so that the bubble growth is essentially thermally-controlled. The superheat varies between $\Delta T_{s,h} = 1.4\text{K}$ and $\Delta T_{s,h} = 5.3\text{K}$, cf. Table 1. Experimentally obtained bubble growth data are available from [11].

Table 1: Initial values for thermally controlled bubble growth.

Symbol	Unit	Case 1	Case 2	Case 3	Case 4	Case 5
$\Delta T_{s,h}$	[°C]	1.4	2.1	3.1	4.5	5.3
$T_{L,0}$	[°C]	101.4	102.1	103.1	104.5	105.3
Δp	[Pa]	5168	5834	11539	17394	20730
t_{c1}	[$\times 10^{-7}$ s]	3.04	5.66	8.78	10.33	11.59
$P_{v,0}$	[Pa]	106492	109158	112863	118718	122054
$P_{G,0}$	[Pa]	5332	7501	11437	15458	22265
$m_{v,0}$	[$\times 10^{-14}$ kg]	2.75	1.00	0.29	0.12	0.04
$m_{G,0}$	[$\times 10^{-15}$ kg]	2.21	1.11	0.47	0.25	0.12
m_E	[$\times 10^{-7}$ kg]	2.21	1.11	0.47	0.25	0.12
$r_{B,0}$	[$\times 10^{-5}$ m]	2.20	1.56	1.02	0.75	0.52
μ_0	[$\times 10^{-8}$]	12.43	9.06	6.14	4.78	3.41

The bubble at rest with initial radius $r_{B,0}$ corresponds to a nucleus and is in unstable equilibrium at the liquid pressure $p_{L,\infty}$ of one atmosphere. This unstable equilibrium is implemented in the simulation by a sudden decrease of initial pressure by $\Delta p = p_{Sat}(T_{L,0}) - p_{L,\infty}$ as described in section 2.3. First, the influence of the variation of the amount of liquid surrounding the bubble is studied (section 3.1), then the non-equilibrium model results are compared to the data and other simulation models (section 3.2).

3.1 Bubble growth in a finite mass of fluid

Case-3 according to Table 1 is chosen for an analysis of the bubble growth for a variation of the elementary cell mass. Since the initial bubble conditions are kept unchanged, this corresponds to a variation of the initial liquid mass. In order to realize a variation of the initial liquid mass alone, for the gas mass fraction x three different values are chose, i.e. $x = 10^{-9}$, $x = 10^{-8}$ (this is the reference according to Case-3 in Table 1) and $x = 10^{-7}$. This rise of x corresponds to a decrease of elementary cell mass from $m_E = 0.4707 \times 10^{-7} kg$ to $m_E = 0.4707 \times 10^{-9} kg$. All other initial conditions are kept constant. From Figure 3 it is obvious that the bubble size (Figure 3(b)) and accordingly the vapor mass (Figure 3(c)) do not grow in an unlimited way but approximate an equilibrium value. This ebbing of bubble growth is due to the decrease of the initial liquid temperature to the bubble temperature (Figure 3(a)) in the course of time so that the driving term in eqn (4) vanishes. Of course, the diminishing strength of the driving temperature difference is due to the assumption that the elementary cell contains a fixed amount of mass and is adiabatic.

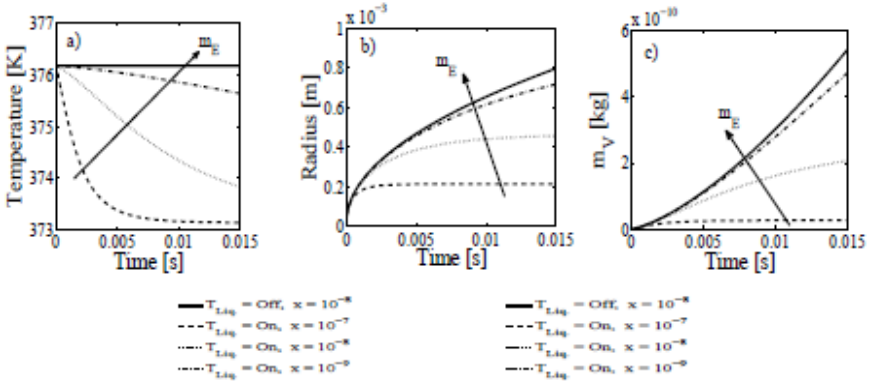


Figure 3: Bubble growth for case-3 and varying elementary cell mass. (a) liquid temperature; (b) radius; (c) vapor mass.

As a limiting case of an infinite amount of surrounding liquid, the liquid temperature T_L is kept constant by switching off the ODE for T_L , eqn (1). This approximation corresponds to an inexhaustible source of energy for bubble growth and to the assumptions made by Plesset and Zwick [4]. As it is

discernible from Figure 3, the results with switched-on ODE for T_L approach this limiting case with increasing elementary cell mass.

In order to assess the performance of the thermal non-equilibrium model for the transition between inertia and thermally controlled growth we choose a dimensionless illustration of the bubble growth according to Mikic *et al.* [15]. In Figure 4, the solutions for varying elementary cell mass are compared to the analytical solution of Mikic *et al.* [15] who assume a zero initial radius. As expected, within the transition phase between the inertia- and thermally-controlled region, the numerical results approach the analytical solution which confirms that the non-equilibrium model is based on assumptions (mechanical non-equilibrium, heat transfer as driving term) that are essentially valid in the thermally controlled regime.

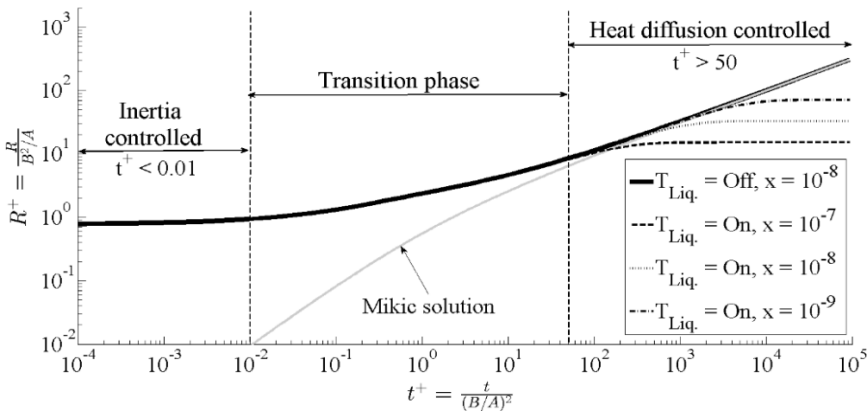


Figure 4: Bubble growth for case-3 in the transition regime.

3.2 Application on thermally-controlled growth

The results of the non-equilibrium model are compared to the analytical solution by Mikic *et al.* [15] and the approximation method of Plesset and Zwick [4] for five superheat levels, cases 1–5 according to Table 1. The initial conditions of both, Plesset–Zwick and non-equilibrium model are equalized. The liquid temperature in the case of Plesset–Zwick theory is a constant value and does not change during the bubble growth, corresponding to a single bubble growth in a large amount of liquid whose mean temperature does not significantly drop due to evaporation and bubble growth. In order to mimic this situation by the thermal non-equilibrium model, the liquid temperature ODE, eqn (1) is switched off and a constant value of $T_L = T_{L,0}$ is applied. We consider a relatively long time interval of t up to 0.015 sec, so that the bubble growth is practically only controlled by heat diffusion within this time interval. In Figure 5 the results of the non-equilibrium model are compared to the ones by the Plesset–Zwick model [4] and the experimental data by Dergarabedian [11].



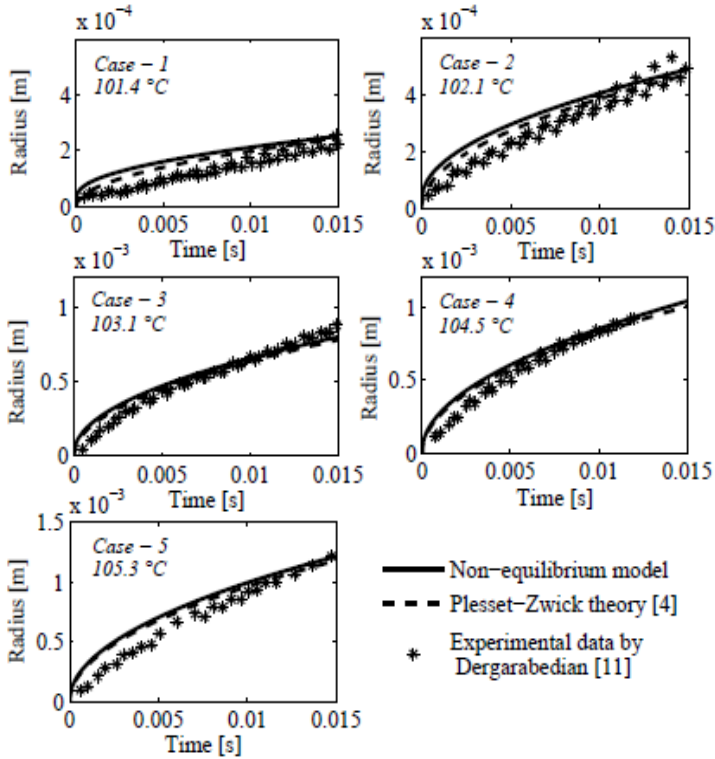


Figure 5: Bubble radius growth for cases 1–5.

The simulation results are rather close to each other. Since several distinct bubbles have been investigated in the experiment, a significant scatter in experimental data is present. This scatter is illustrated by star symbols whose deviation is in the same order of magnitude as the difference of the simulation results to the experimental mean value. Furthermore, Dergarabedian [11] specifies an uncertainty in the time instant where the bubble starts to grow of 0.001 sec. Taking this into account, we conclude that the agreement between simulation data and experiment is good. In particular, the thermal non-equilibrium model performs equally well as the well-established model by Plesset and Zwicky [4].

4 Conclusions

We have analyzed the thermal non-equilibrium model of Iben [19, 20] for bubble growth in superheated liquids and have shown that it performs equally well as the solution by Mikic *et al.* [15] and Plesset and Zwicky [4] in the heat diffusion controlled range. Therefore, for superheated liquids at high temperatures, where

the critical time is very small so that thermal effects dominate the bubble growth for almost the entire growth process, the non-equilibrium model is an equivalent alternative to Rayleigh–Plesset based models as the Plesset–Zwick [4] model. The advantage of the non-equilibrium model will be revealed if it is implemented in 3D-CFD codes. The embedding of a bubble in a finite amount of surrounding liquid and the harmless numerical properties are expected to be advantageous. The definition of a fixed elementary cell mass may mimic a computational CFD cell, so that the model is assumed to be well suitable for a straightforward implementation in 3D-CFD codes which will be done in future works. Of course, the model will need to be reformulated for a fixed volume instead of a fixed mass to be consistent with common finite volume approximations of the 3D governing equations.

Acknowledgements

The authors thank the “Forschungsschule Energieeffiziente Logistik” for financial support on the scholarship of the first author and Dr. Uwe Iben for several helpful discussions on the model implementation.

References

- [1] Nigmatulin, R.I., Basics of the mechanics of the heterogeneous fluids, Nauka: Moskva, 1978.
- [2] Beylich, A.E., Dynamics and thermodynamics of spherical vapor bubbles. *Int. Chem. Eng.*, **31(1)**, pp. 1–28, 1991.
- [3] Matsumoto, Y. & Takemura, F., Influence of internal phenomena on gas bubble motion. *JSME International Journal*, **37(2)**, pp. 288–296, 1994.
- [4] Plesset, M.S. & Zwick, S.A., The growth of vapor bubbles in superheated liquids. *J. Appl. Phys.*, **25(4)**, pp. 493–450, 1954.
- [5] Forster, H.K. & Zuber, N., Growth of a vapor bubble in a superheated liquid. *J. Appl. Phys.*, **25(4)**, pp. 474–478, 1954.
- [6] Scriven, L.E., On the Dynamics of Phase Growth. *Chem. Eng. Sci.*, **10**, pp. 1–13, 1959.
- [7] Fritz, W. & Ende, W., Über den Verdampfungsvorgang nach kinematographischen Aufnahmen an Dampfblasen. *Physik Zeitschrift*, **37**, pp. 391–401, 1936.
- [8] Hooper F.C. & Abdelmessih, A.H., 3rd Int. Heat Tr. Conf., Chicago, 1966.
- [9] Cole, R. & Shulman, H.L., Bubble growth rates at high Jakob numbers. *Int. J. Heat Mass Transfer*, **9**, pp. 1377–1390, 1966.
- [10] Bankoff, S.G., Asymptotic growth of a bubble in a liquid with uniform initial superheat. *Appl. Sci. Res. A*, **12**, pp. 267–281, 1964.
- [11] Dergarabedian, P., The rate of growth of vapor bubbles in superheated water. *ASME J. Appl. Mech.*, **20**, pp. 537–545, 1953.
- [12] Plesset, M.S., The dynamics of cavitating bubbles. *ASME J. Appl. Mech.*, **16**, pp. 228–231, 1949.



- [13] Rayleigh, L., On the pressure developed in a liquid during the collapse of a spherical cavity. *Phil. Mag.*, **34**, pp. 94–98, 1917.
- [14] Brennen, C.E., *Cavitation and Bubble Dynamics*, Oxford University Press: California, 1995.
- [15] Mikic, B.B., Rohsenow, W.M. & Griffith, P., On bubble growth rates. *Int. J. Appl. Heat Mass Transfer*, **16**, pp. 657–666, 1969.
- [16] Sauer, J. & Schnerr, G.H., Unsteady cavitating flow - A new cavitation model based on a modified front capturing method and bubble dynamics. *Proceedings of the ASME fluid engineering division summer meeting*, Boston, 2000.
- [17] Kubota, A., Kato, H. & Yamaguchi, H., A new modeling of cavitating flows: a numerical study of unsteady cavitation on a hydrofoil section. *Journal of Fluid Mechanics*, **240(1)**, pp. 59–96, 1992.
- [18] Preston, A.T., Colonius, T. & Brennen, C.E., A numerical investigation of unsteady bubbly cavitating nozzle flows. *Physics of Fluids*, **14(1)**, pp. 300–311, 2001.
- [19] Iben, U., *Modeling of Cavitation. Systems Analysis Modelling Simulation*, **42**, pp. 1283–1307, 2002.
- [20] Iben, U., *Entwicklung und Untersuchung von Kavitationsmodellen im Zusammenhang mit transienten Leitungsströmungen*, VDI-Verlag: Düsseldorf, 2004.
- [21] Epstein, P.S. & Plesset, M.S., On the stability of gas bubbles in liquid-gas solutions. *J. Chemical Physics*, **18 (11)**, pp. 1505–1509, 1950.
- [22] Klein, A. & Iben, U., Modelling of Air release in Liquids. 7th Int. Conference on Heat Transfer, Fluid Dynamics and Thermodynamics (HEAT2010), Ankara, Turkey, 19–21 July 2010.
- [23] Wagner, W. & Pruss, A., The IAPWS formulation 1995 for the thermodynamic properties of ordinary water substance for general and scientific use. *J. Phys. Chem.*, **31(2)**, pp. 387–535, 2002.
- [24] Span, R., *Multiparameter equations of state – An accurate source of thermodynamic property data*, Springer: Berlin, 2000.
- [25] MATLAB, The MathWorks Inc., Version R2012, Natick (MA), 2012.

